Available online at www.sciencedirect.com
SCIENCE DIRECT
Biochimica et Biophysica Acta 1763 (2006) 561 – 575
BIOCHIMICA ET BIOPHYSICA ACTA
BBA
http://www.elsevier.com/locate/bba

Review

High resolution imaging of live mitochondria

Stefan Jakobs *

Max-Planck-Institute for Biophysical Chemistry, Department of NanoBiophotonics, Mitochondrial Structure and Dynamics Group, Am Fassberg 11, 37077 Goettingen, Germany

Received 16 January 2006; received in revised form 12 April 2006; accepted 13 April 2006
Available online 20 April 2006

Abstract

Classically, mitochondria have been studied by biochemical, genetic and electron microscopic approaches. In the last two decades, it became evident that mitochondria are highly dynamic organelles that are frequently dividing and fusing, changing size and shape and traveling long distances throughout the life of a cell. The study of the complex structural changes of mitochondria in vivo became possible with the advent of fluorescent labeling techniques in combination with live cell imaging microscopy. This review aims to provide an overview on novel fluorescent markers that are used in combination with mitochondrial fusion assays and various live cell microscopy techniques to study mitochondrial dynamics. In particular, approaches to study the movement of mitochondrial proteins and novel imaging techniques (FRET imaging-, 4Pi- and STED-microscopy) that provide high spatial resolution are considered.

Keywords: FRAP; FLIP; Fluorescence microscopy; Fusion assay; Mitochondria; Photoactivation; Self labeling protein tag

1. Introduction

Since the identification of mitochondria by electron microscopy in the 1950s, it has been become clear that sometimes mitochondria exist as a single elaborate network and at other times they become fragmented [1–3]. Mitochondria continuously move, divide and fuse in a highly regulated fashion. The investigation of the close relationship of mitochondrial dynamics with numerous cellular processes as documented in this special issue would not have been possible without the use of fluorescence microscopy as a tool to visualize mitochondrial dynamics in vivo.

Next to the mitochondrial dynamics at the level of the whole network, the mitochondrial inner structure is reorganized upon various stimuli [4]. Comparatively little data are available on the movement of proteins within mitochondria and even less is known about the regulation of inner-mitochondrial protein movement; likely, live cell microscopy will be an indispensable tool to elucidate this level of mitochondrial dynamics.

The enormous popularity of live cell imaging has been driven by the advancements in two fields: The advent of fluorescent probes to specifically label individual proteins and the development of an array of microscopic technologies to image live cells in time and space. Excellent in-depth descriptions of commonly used widefield, confocal and deconvolution systems as used in many laboratories are given elsewhere (see [5,6] and references therein). This review highlights some of the past achievements and briefly discusses the current and emerging technologies and strategies that are, or may be, used to visualize mitochondrial dynamics in vivo. Although this review focuses on the application of these techniques to the analysis of mitochondria, most of the described approaches are evidently equally well suited to look into other cellular compartments.

Abbreviations: aa, amino acid; BFP, blue fluorescent protein; BG, benzylguanine; CFP, cyan fluorescent protein; FCS, fluorescence correlation spectroscopy; FLIP, fluorescence loss in photobleaching; FP, fluorescent protein; FRAP, fluorescence recovery after photobleaching; FRET, fluorescence resonance energy transfer; GFP, green fluorescent protein; MMM-4Pi, multifocal multiphoton 4Pi microscopy; RESOLFT, reversible saturable optical fluorophore transitions; RSFP, reversible switchable fluorescent protein; PAFP, photoactivatable fluorescent protein; STED, stimulated emission depletion; YFP, yellow fluorescent protein

* Tel.: +49 551 201 2531; fax: +49 551 201 2505.
E-mail address: sjakobs@gwdg.de.

0167-4889/$ - see front matter © 2006 Elsevier B.V. All rights reserved.
doi:10.1016/j.bbamcr.2006.04.004

2. Stains

Mitochondria are generally difficult to visualize using phase contrast or differential interference contrast optics. Hence over the last decades several vital stains have been identified to specifically label mitochondria in live cells. The uptake of most of these dyes into mitochondria is dependent on an intact mitochondrial membrane potential. Some of the mostly positively charged, lipophilic fluorescent dyes change their fluorescence emission depending on the immediate environment and may therefore be used to make qualitative, or even quantitative, measurements of mitochondrial membrane potential. The use and properties of such stains are expertly covered elsewhere [7–9]. Table 1 provides an overview of the commonly used vital stains for mitochondria.

However, since these stains label mitochondria or their membranes on the whole, they are generally not suitable for the microscopic investigation of the spatial and temporal dynamics of specific mitochondrial proteins. This task has become feasible with the discovery of the green fluorescent protein (GFP) isolated from the jellyfish *Aequorea victoria*.

3. Fluorescent proteins

GFP was discovered more than 40 years ago [16,17], but it was not until the cloning and heterologous expression of the GFP gene in the early 1990s [18–20], that it attracted widespread interest. Briefly after its cloning GFP has been used to visualized mitochondria in live cells [21]. Since then, a whole panel of further fluorescent proteins (FPs) have been discovered, or generated by mutagenesis, that cover almost the entire visible spectrum [22,23].

A. victoria GFP is a monomer with a weak tendency to form dimers. Many subsequently found naturally occurring FPs including the red fluorescent DsRed from the coral *Discosoma* sp., have a strong tendency to form tetramers. When used as a fusion tag, such a tendency for tetramerization is generally a major problem, since it is likely to interfere with the functionality of the host proteins. Still, this disadvantage has been exploited. DsRed's tendency to form tetramers was used to enforce aggregation of the mitochondrial F_1F_0-ATPases in yeast cells [24]. DsRed, when fused to Atp3, the γ-subunit of the F_1F_0-ATPase, results in cross-linking of the ATP synthase complexes in vivo, which in turn induces the absence of cristae, indicating an important role of the ATP synthase complexes for the maintenance of the mitochondrial inner structure.

To eliminate the DsReds' tetramerization tendency, extensive mutagenesis has been performed [22,25]. As a result, monomeric FPs with emission spectra covering almost the entire visible spectrum are now available. For a practical guide to choose the appropriate FP for an experiment, see [26].

Besides the use as 'molecular bulbs', substantial efforts have been undertaken to develop FP-based sensors to monitor various cellular parameters like pH, redox potential, Ca^{2+} or Cl^- concentrations [23,27,28]. In an early report, a pH-sensitive FP-based sensor (GFP-F64L/S65T) was targeted to the mitochondrial matrix of CHO cells [29]. However, expression of this probe did not allow accurate determination of the matrix pH value because of its low pK_a. This limitation was soon alleviated by the development of new pH sensitive FPs [30–32]. Abad et al. generated the GFP-based pH indicator mtAlpHi, that has an apparent pK_a of ~8.5 and that exhibits changes in fluorescence intensity upon pH shifts. Using mtAlpHi, the authors determined a matrix pH of around 8.0 in resting HeLa cells. After challenging the cells with various compounds, such

Table 1
Vital stains for mitochondria

Stain	Comments	Excitation maximum (nm)	Emission maximum (nm)
$DiOC_6$ (3, 3′-Dihexyloxacarbocyanine iodide)	Stain for mitochondria. Also used as a potentiometric dye for assessment of the mitochondrial membrane potential $\Delta\Psi_m$. Stains at higher concentrations the endoplasmic reticulum. Like Rhod 123, $DiOC_6$ may inhibit mitochondrial respiration [10].	488	501
JC-1 (5,5′,6,6′-Tetrachloro-1,1′,3, 3′-tetraethylbenzimidazolylcarbocyanine iodide)	Ratiometric indicator for assessment of $\Delta\Psi_m$. The dye exists in two different states with different emission spectra depending on the concentration. The spectral shift occurs upon aggregate formation within the mitochondrial matrix that is dependent on dye concentration, which in turn is dictated by $\Delta\Psi_m$ [9,11,12].	514	527 and 590
MitoTracker and MitoFluor probes	A series of mitochondrial specific stains with different properties. For details see [13].		
NOA (Nonyl acridine orange)	NOA binds to cardiolipin. Uptake into mitochondria is apparently not dependent on membrane potential [14]. The dye has been used for long term studies.	495	522
Rhod 123 (Rhodamine 123)	Sequestered by active mitochondria. Historically, this dye has been very popular to monitor $\Delta\Psi_m$. Several limitations have to be considered when using this dye for the assessment of membrane potential [8].	507	529
TMRE (Tetramethylrhodamine ethyl ester) and TMRM (Tetramethylrhodamine methyl ester)	Both dyes are structurally very similar to Rhod 123. May be used as potentiometric dyes for the assessment of $\Delta\Psi_m$ [9,15]. Both have been reported to inhibit respiration, with TMRE being the more potent inhibitor. These compounds are more membrane permeable than Rhod 123.	549 (548)	574 (573)

as the Ca^{2+} inonophores ionomycin or A23187, a matrix acidification was recorded [31]. Using the yellow fluorescent EYFP as a pH-sensitive probe, Porcelli et al. came to a similar value (~7.8) for the matrix pH in resting ECV304 cells and estimated the pH in the intermembrane space to be around 6.9 [32]. The redox-sensitive ratiometric probe roGFP targeted to the mitochondria of HeLa cells revealed a highly reducing matrix, with a midpoint potential near −360 mV [33]. Likewise, tremendous progress has been achieved in measuring Ca^{2+} concentrations in live cells using genetically-encoded fluorescent indicators based on various GFP variants (camgaroo, pericam, and cameleon probes, see [34] and references therein).

Recently, a comprehensive collection of budding yeast (*Saccharomyces cerevisiae*) strains expressing full-length, chromosomally tagged GFP-fusion proteins has been generated [35]. In this study, 527 GFP tagged proteins were microscopically identified to be localized to the mitochondria. Although some of these fusion proteins might be mislocalized due to the fusion tag, it can be concluded that more than 50% of the up 1000 mitochondrial yeast proteins [36–39] can be C-terminally tagged with GFP and visualized. It should be noted, however, that many of these GFP tagged proteins are only weakly expressed from their endogenous promoters; hence visualization of such fusion proteins might prove to be a technical challenge. And, of course, proper localization does not necessarily imply full functionality of the fusion protein. Those mitochondrial proteins that do not tolerate a C-terminal FP tag likely require more elaborate cloning strategies, since the common N-terminal targeting signals of mitochondrial proteins frequently impair N-terminal fusions.

Aside from the cloning problems, two possible shortcomings might be associated with the use of FPs: Their rather large mass of ~28 kDa, and their limitation to a single, genetically encoded function. Several GFP-independent tagging strategies have been emerging recently to tackle these potential shortcomings.

4. Tag-mediated in vivo labeling of fusion proteins with small molecules

Alternative strategies that are based on a tag-mediated labeling of fusion proteins with synthetic (fluorescent) molecules have been covered by several excellent reviews [40–44]. Because of the numerous reviews on this topic, only three commercially available tag-mediated labeling systems will be briefly discussed here.

The first approach to specifically label fusion proteins with synthetic molecules was the biarsenical tetracysteine method introduced by the Roger Tsien laboratory [45]. It is based on the formation of stable complexes between biarsenical compounds such as the green fluorescent FlAsH or the red fluorescent ReAsH to peptides containing the tetracysteine motif Cys–Cys–Pro–Gly–Cys–Cys [45,46] (Fig. 1A). FlAsH and ReAsH are sold as LumioGreen and LumioRed (www.invitrogen.com). The tetracysteine motif that may be as small as 6 amino acids is potentially less perturbative than the incorporation of a FP [47–49], thus this method elegantly combines the advantages of site-specificity with a small tag.

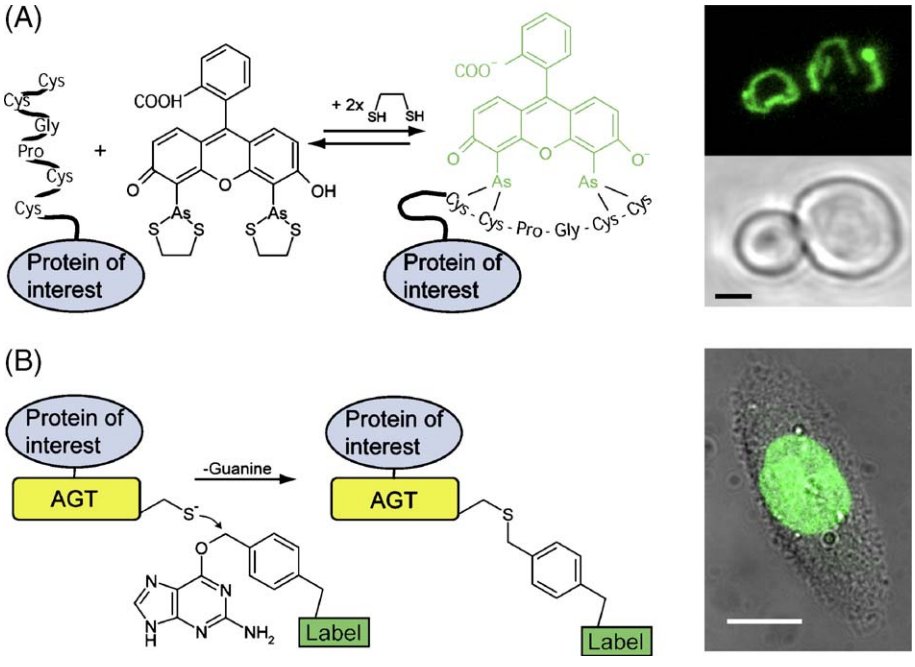

Fig. 1. Tag-mediated labeling with small molecules. (A) The biarsenical tetracysteine system. Left: a biarsenical compound (e.g., FlAsH) binds to the tetracysteine motif (the short peptide CCPGCC) that is fused to the protein of interest. Right: budding yeast cell expressing a matrix targeted fusion protein labeled with FlAsH. Displayed is a bright field image (bottom) and a maximum intensity projection of individual confocal sections (top). Scale bar: 2 μm. (B) Left: covalent labeling of AGT (O^6-alkylguanine-DNA alkyltransferase) fusion proteins with benzylguanine (BG) derivatives. Right: confocal image of a transiently transfected CHO cell expressing a nuclear targeted AGT fusion protein labeled with a fluorescent BG derivative. Displayed is an overlay of the transmission and the fluorescence channel. The image is a courtesy of A. Keppler and K. Johnsson. Scale bar: 10 um.

Besides, the currently available biarsenical-tetracysteine labels offer additional potential applications, including correlative fluorescence and electron microscopy, and chromophore-assisted light inactivation for spatially restricted inactivation of proteins. Reportedly, a potential disadvantage of the method is strong nonspecific binding of the fluorophores, frequently observed in mammalian cell culture cells [50,51]. In budding yeast, however, very low non-specific staining was observed [48]. The Tsien group optimized the flanking sequences of the tetracysteine motif, thus further improving the affinity of the tag for biarsenical compounds [52]. The tetracysteine tagged α subunit of the mitochondrial F_1F_0 ATP synthase (Atp1) was visualized in live budding yeast cells after labeling with FlAsH [48]. We have used ReAsH and FlAsH to label several mitochondrial proteins for time-lapse microscopy (C. Wurm, M. Andresen, S. Jakobs, unpublished). Hence the system is clearly suitable for the labeling of mitochondrial proteins, at least in yeast. However, since FlAsH and ReAsH are both prone to photobleaching, their suitability for extended time-lapse imaging or visualization of rare proteins has still to be evaluated.

Other strategies for tag-mediated protein labeling involve covalent labeling of fusion proteins in vivo. Kai Johnnson's group reported that benzylguanine (BG) derivatives can be used to irreversibly and specifically label proteins fused to human O^6-alkylguanine-DNA alkyltransferase [53–55] (Fig. 1B). This tag has a size of 182 amino acids (aa), so it is slightly smaller than GFP (238 aa), but much larger than a tetracysteine motif tag (6 aa). This approach has been successfully employed to label proteins in different compartments of mammalian cell lines [55] as well as in the nucleoplasm of the microaerotolerant protozoan parasite *Giardia intestinalis* [56]. To our knowledge, no labeling of mitochondrial proteins with BG derivatives has been reported as yet. Several fluorescent BG derivatives are commercially available (Snap-tag; www.covalys.com).

A conceptually similar strategy (Halo-tag; www.promega.com) is based on the use of a halogen dehalogenase from the bacterium *Rhodococcus rhodochrous* as a tag. Neither eukaryotic cells nor *E. coli* possess alkyl dehalogenases, so specific covalent labeling is likely to be possible in many organisms. However, with 293 aa, the tag is rather large and the approach has not been evaluated for many applications.

Despite their obvious potentials, none of the tag-mediated in vivo labeling strategies have found widespread use for the visualization of cellular proteins (not to speak about mitochondrial proteins) as yet. Hence, this review focuses on the imaging of mitochondrial FP-fusion proteins.

5. Imaging mitochondrial motion

Mitochondria are highly dynamic organelles. Their movement has been imaged from the level of the mitochondrial network as a whole down to the intrinsic movement of single enzymes or protein complexes. Some of the microscopic strategies that are used for the recording of these movements, which may differ in the examined time scales or distances by several orders of magnitude, will be highlighted in the following.

6. 4D imaging

Mitochondria form highly dynamic interconnected tubular networks that continually change their position and shape and travel long distances on cytoskeletal tracks [1,2]. The spatiotemporal dynamics of the mitochondrial network in mammalian cells [21,57–59], plants [60,61], yeast [3,62–64], or in programmed cell death [59,65,66] has been investigated in numerous studies.

The most complete representation of the dynamic and spatially complex structure of mitochondria is achieved by recording the image data in three spatial dimensions over time (four-dimensional (4D) imaging) [67,68]. For a comprehensive review on the technical requirements for 4D microscopy see [69] and references therein. Currently, most studies on mitochondrial dynamics rely either on widefield fluorescence or various types of confocal laser-scanning microscopy.

The image data recorded with widefield fluorescence microscopes have inevitable a poor optical resolution along the z axis. To partly compensate for this drawback, widefield data-sets are frequently deconvolved to provide a better spatial resolution in the final 4D stacks. The deconvolution requires, next to a sufficient signal-to-noise ratio and a good knowledge of the intensity distribution in the focus, some computational efforts. Confocal laser scanning microscopes, in contrast, excite the fluorophores by moving a single focus (in case of point scanning systems) or an array of foci (spinning-disk systems) over the specimen. Confocal microscopes detect only fluorescence from the focal plane by rejecting the out-of-focus blur, thus performing optical sectioning by physical means. Hence confocal microscopes generate spatial resolution along the z-axis without the need of computer-assisted deconvolution (although it is possible and often advisable to deconvolve confocal data-sets to further increase the attained resolution in the final images). With confocal microscopes the attainable resolution within the optical plane is only slightly higher, if at all visible, compared to widefield microscopy. Their predominant advantage is the removal of out of focus blur.

A major concern in 4D live cell imaging is the limited number of photons that can be acquired from a specimen. A single FP typically undergoes on average 1.3×10^4 to 10^5 absorption cycles until it is irreversibly photobleached [70]. Therefore, the number of fluorescence images that can be taken from a cell is ultimately limited. Increasing numbers of FP-fusion proteins targeted to a mitochondrion may increase the maximum amount of obtainable images. However, overexpression of functional fusion proteins frequently has an influence on mitochondrial structure. Similarly, high level expression of FPs fused to targeting sequences for the inner or outer membrane often interferes with mitochondrial morphology. Nonetheless, mitochondria seem to tolerate very high levels of freely diffusing FPs in the matrix. Hence most studies analyzing mitochondrial network dynamics over extended time periods relied on FPs targeted to the mitochondrial matrix, typically by

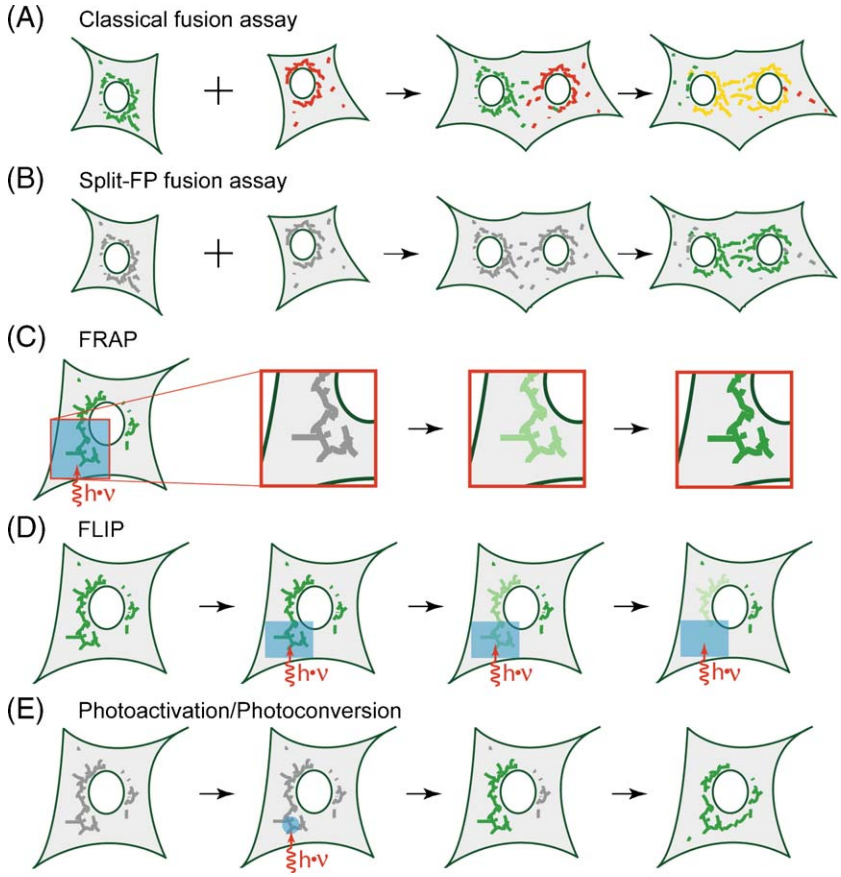

Fig. 2. Strategies to record protein movement within mitochondria. (A) Classical fusion assay. The mitochondria of two cells are labeled with two different fluorophores (e.g., GFP and DsRed). Upon cell fusion the intermixing of the fluorophores is recorded over time. (B) Proposed split-FP fusion assay. The non-fluorescent N- and C-terminal fragments of a FP are targeted to the matrices of different cells. Upon fusion of the cells and subsequent intermixing of the matrix contents, both fragments assemble to a fluorescent protein. The intermixing of the matrix contents results in the de-novo generation of a fluorescence signal. (C) FRAP. The fluorescence signal of FP-fusion proteins within a spatially defined region is irreversibly photobleached by intense laser light ($h\cdot\nu$). Subsequently FP-fusion proteins from the non-bleached regions move into the bleached region. The recovery of fluorescence within this region is recorded by imaging with low light intensities. (D) FLIP. Within a spatially defined region mitochondrial targeted FPs are continuously photobleached with intense light ($h\cdot\nu$). The fluorescence in the rest of the cell is simultaneously recorded with low light intensities. In the latter region, a decrease in the fluorescence signal is due to the connectivity to mitochondria of the bleached region. (E) Photoactivation/Photoconversion. Mitochondrial targeted photoactivatable proteins (e.g., PAGFP or Kaede) are highlighted by a pulse of intense laser light in a spatially defined region ($h\cdot\nu$). Subsequently the movement of the highlighted proteins is followed over time.

fusion of the FPs to the presequences of human cytochrome *c* oxidase subunit VIII, yeast Cox4 or subunit 9 of the *Neurospora crassa* F_0-ATPase [21,71,72].

Although time-lapse microscopy is an extremely powerful tool to follow the dynamic changes of a mitochondrial network as a whole, it often fails to distinguish between tubule fusion and close spatial proximity of tubules, or to monitor the movement of tagged proteins within mitochondria. To overcome these limitations, a number of additional strategies have been developed.

7. Fusion assay

An elegant assay for mitochondrial mixing in budding yeast cells was developed by Nunnari and colleagues [3]. In the original experiments, mitochondria in haploid cells of opposite mating types are labeled with either a mitochondrial matrix targeted GFP or a mitochondrial-specific red fluorescent vital dye. Subsequently, the intermixing of the two mitochondrial labels is monitored microscopically during mating of the cells. It was found that the parental mitochondrial proteins were redistributed rapidly throughout the zygotes, providing unequivocal evidence that mitochondria fuse and that their contents intermix. Soon after the discovery of DsRed, a matrix targeted variant of this red fluorescent protein was utilized to replace the red fluorescent vital dye in the assay [73,74]. Since its first description, the fusion assay has been widely used to functionally characterize proteins involved in mitochondrial fusion, fission and inner membrane remodeling in yeast (e.g., [75–79]).

Similar fusion assays have been developed for plant protoplast [80] and for human cell lines [81,82]. For mammalian cell lines, as in the yeast assay, cells carrying differently labeled mitochondria were mixed and plated on glass coverslips. Cell fusion was induced by treatment with polyethylene glycol [81,83,84] or by using a hemagglutinating virus [82] (Fig. 2A). These studies showed that mitochondrial fusion in human cells is efficient, and that complete intermixing

of the matrix contents is achieved in less than 12 h [81]. Fusion of mammalian mitochondria requires an intact mitochondrial inner membrane potential but is independent of a functional cytoskeleton [84].

Fusion assays are not restricted to the use of matrix-targeted FPs, but have also been carried out with markers targeted to other mitochondrial sub-compartments such as the inner and outer membranes. By employing this strategy, Malka et al. demonstrated that in human cells, fusion of inner and outer membranes are separate events in vivo [85].

8. FP-fragment reassembly

Most fluorescent proteins, when split into an N- and a C-terminal fragment do not associate to give a reassembled FP upon co-expression. Remarkably, however, if the fragments are fused to strongly interacting protein domains, like for example antiparallel leucine zippers, association and fluorescence of the split FP are achieved in vivo [86–88]. The fluorescence signal of the re-associated split FP is a very sensitive measure for interactions of the domains because a functional fluorophore is only generated after the protein domain assisted association of the two FP-fragments. Variations of this scheme have been used to study protein–protein interactions based on split GFP [86,89] or split CFP and split YFP [87,90–92].

Cabantous et al. have engineered soluble fragments of GFP that self-associate without the requirement for interacting fused domains [93]. Neither fragment on its own is fluorescent. When mixed, the small and the large GFP fragment spontaneously associate, resulting in GFP folding and formation of the fluorophore. It can easily be anticipated that the two split GFP fragments may be targeted to the mitochondrial matrices of different cells. Upon cell fusion, the fusion of the mitochondrial networks would be detectable by a de novo fluorescence signal of the associated split-GFP (Fig. 2B). This is expected to give a very sensitive readout measure, because the signal-to-noise ratio (in this case a fluorescence signal versus no fluorescence) is likely to be very favorable. Although this variant of a fusion assay has not been, to our knowledge, experimentally realized as yet, we propose that the use of a split-GFP system is an interesting alternative to monitor mitochondrial fusion.

Apart from mere analyzing mitochondrial fusion, these cellular assays might be combined with functional FP-fusion proteins to investigate the movement of specific protein complexes within mitochondria. However, the requirement for chemically induced cell fusion in mammalian cells precludes data collection under normal growth conditions or during dynamic changes of growth conditions. Hence alternative strategies to investigate the movement of FP labeled proteins within mitochondria in vivo may rely on the spatially defined deliberate photobleaching of FP fluorescence.

9. Fluorescence recovery after photobleaching

Fluorescence recovery after photobleaching (FRAP) has been developed in the pre-GFP era to investigate the diffusion of molecules in living cells [94–98]. This strategy has witnessed a renaissance after the introduction of GFP and commercially available confocal microscopes [99–102]. FRAP is now frequently used to determine the intracellular movements of tagged proteins provided the motion is over distances resolvable by light microscopy.

In its classical form, a region of interest is selectively photobleached using intense laser light and the recovery that occurs as molecules move into the bleached region is monitored over time with low intensity excitation light (Fig. 2C). Careful analysis of the fluorescence recovery in the photobleached region can provide information on the diffusion constant, transport rate, mobile/immobile fraction, or binding/dissociation rates of the FP-tagged protein. A number of variations of this scheme have been successfully applied, including inverse FRAP (iFRAP), where the molecules outside a region of interest are photobleached and the loss of fluorescence from the non-photobleached region is monitored over time [100,103]. Another variation is fluorescence loss in photobleaching (FLIP). In FLIP experiments, a small region of interest is repeatedly photobleached with high light intensities while the rest of the cell is imaged with low light intensities (Fig. 2D). This approach is particularly suited to determine the connectivity of mitochondrial networks. In a FLIP experiment, those parts of the network that are luminally connected to the region being bleached gradually lose fluorescence due to lateral movement of mobile FP tagged proteins.

Surprisingly, the discussion on mitochondrial connectivity – Do mitochondria exist as discrete organelles within the cells or is the mitochondrial network a contiguous entity similar to the endoplasmic reticulum?– has not resulted in a consensus yet. Luminal continuity of the mitochondrial compartment likely has far reaching consequences on many cellular processes. A luminally contiguous mitochondrial network would possibly allow 'Ca^{2+} tunneling' akin to the ER throughout the cell [104]. Furthermore, an electrically continuous mitochondrial network may allow 'energy transmission' across the cell [105].

Using non-confocal deconvolution imaging in combination with long-term (30 min) FRAP experiments, Rizzuto et al. observed a largely connected, continuous mitochondrial network in HeLa cells [106]. These early findings have later been contradicted by other FRAP studies on several human cell lines including HeLa, employing shorter time-scales, pointing to mitochondria that exist in separate entities at a given point in time [58,107]. Similarly, photobleaching experiments on pancreatic acinar cell revealed distinct groups of mitochondria that were not luminally connected [108]. Apparently, the level of mitochondrial connectivity varies substantially between cell types and upon environmental conditions.

FRAP has an enormous, albeit in the mitochondrial field largely disregarded potential to investigate the diffusion kinetics of functional tagged proteins. Partikian et al. demonstrated that GFP targeted to the mitochondrial matrix of mammalian cells has diffusion coefficients of $2–3 \times 10^{-7}$ cm^2 s^{-1}, which is only 3- to 4-fold less than that for GFP in water [109]. Hence somewhat surprisingly, the infoldings of the cristae do not pose a major obstacle for the free diffusion of matrix proteins. In fact, the observed unobstructed diffusion is in line with computer

simulations predicting that barriers introduced by cristae would have only minor effects on the diffusion rates [110]. However, the mitochondrial matrix appears to be the most crowded aqueous cellular compartment with protein concentrations larger than 300 mg protein/ml [111,112]. Such a high protein concentration is expected to severely reduce free diffusion. Hence, an intriguing possibility for the observed fast GFP diffusion in the matrix is that a large proportion of the matrix resident proteins are organized in membrane associated clusters, leaving a relatively protein-free matrix that allows free diffusion of solutes. In line with this argument, two subunits of the fatty acid β-oxidation multienzyme complex residing in the matrix were observed to be essentially immobile [109]. Furthermore, FRAP-analysis of four proteins involved in the tricarboxylic acid cycle (malate dehydrogenase, citrate synthase, isocitrate dehydrogenase and succinyl-CoA synthetase) revealed similar diffusion rates, despite different molecular weights of the individual proteins. Each of these four proteins were found partly in an apparently immobile pool and partly in a mobile pool with a diffusion coefficient ~4-fold lower than that of unconjugated GFP [113]. Such a 4-fold slowed diffusion rate indicates that the respective proteins are associated in a large macromolecular complex of ~1.7 MDa.

To our knowledge, no data on the mobility of mitochondrial integral membrane proteins have been published so far. It is easy to predict that many surprises on the regulation of the diffusive behavior of mitochondrial proteins await their discovery.

10. Photoactivatable proteins

Photoactivation, as opposed to photobleaching, is a complementary strategy to FRAP to visualize protein dynamics in live cells. It works by converting a photoactivatable fluorescent protein (PAFP) in a (different) fluorescent state through irradiation with a brief high-intensity light pulse (for review, see [100,114]). Some PAFPs convert from a dark to a fluorescent state, whereas others change their emission spectrum. They may be tagged to a host protein, as any other FP, creating a functional photoactivatable fusion protein. After highlighting PAFPs in a spatially defined region of the cell, generally by using a confocal microscope, the molecules can be followed as they re-equilibrate in the cell over time (Fig. 2E). Similar to FRAP-experiments, these time-lapse data may be used to determine kinetic parameters like the transport rate or binding/dissociation rates of the PAFP-tagged protein. The data from photoactivation experiments are generally easier to interpret than FRAP results, because after photoactivation the fate of proteins highlighted at a defined region at a specific time-point is analyzed. However, the measured fluorescence signal in FRAP experiments is often larger, resulting in better signal-to-noise ratios.

PAFPs have been discovered only recently, hence few published studies relied on these fluorescent markers to study mitochondrial protein dynamics so far. Under low oxygen conditions, the well known GFP from *Aequorea victoria* and several of its variants can be used as a PAFP, because under these conditions GFP is transferred by irradiation with blue light from the green into a brightly red fluorescent state [115,116]. Using photoconversion of matrix targeted GFP, it was demonstrated that in logarithmically growing yeast cells the mitochondrial compartment is generally luminally contiguous. Occasional small independent fragments fuse within a few minutes to the large compartment, resulting in a rapid intermixing of the mitochondrial matrix [117]. However, this green-to-red transition of GFP has only limited applications, because low oxygen conditions are required so it can only be used in facultative anaerobic organisms like budding yeast. Hence in later studies PAFPs without this limitation have been used to study mitochondrial connectivity [118,119]. PAGFP is a variant of the *A. victoria* GFP that, after irradiation with intense light of near 400 nm, increases its green fluorescence ~100 times [120]. Using matrix targeted PAGFP, Karbowski et al. quantitated mitochondrial fusion rates in cultured mammalian cells. They were able to demonstrate that during apoptosis mitochondrial fusion is blocked independently of caspase activation and they conclude that this block may be a consequence of Bax/Bak activation during apoptosis [119]. To visualize mitochondrial fusion in plant cells, Arimura and colleagues employed Kaede, which has been originally cloned from the stony coral *Trachyphyllia geoffroyi* [121]. In its ground state Kaede exhibits green fluorescence that can be converted to red by irradiation with intense UV light. Interestingly, they report that in onion epidermal cells mitochondrial fission is not necessarily accompanied by an equal distribution of the mitochondrial DNA, resulting in mitochondria containing various amounts of DNA within a single cell [118]. Frequent and transient fusion of mitochondria might be required to overcome the heterogeneity of DNA contents in plant mitochondria.

Photobleaching, and even more photoactivation, require relatively high expression levels of the tagged protein to provide a sufficient signal-to-noise ratio. Hence, these techniques are largely unsuited for the analysis of rare fusion proteins.

11. Fluorescence correlation spectroscopy (FCS)

In contrast to photoactivation/photobleaching strategies, FCS [122–124] requires only low (nanomolar or even lower) concentrations of the tagged proteins. FCS is an optical technique with single-molecule sensitivity that extracts information from fluctuations in molecule concentrations within the microscope focus. Hence FCS does not require overexpressed proteins, so it is well suited to collect data under physiological conditions. Based on the detection of fluctuations from single fluorescent molecules or proteins moving in and out of a diffraction-limited laser focus, as it can be generated in a confocal microscope, FCS has been successfully used to resolve particle dynamics within living cells (for review, [125–128]). FCS requires substantial mathematics analysis to extract the information from the obtained fluorescence fluctuation data, which is well established but generally non-trivial. Various promising conceptual extensions of FCS have been described, including

fluorescence cross-correlation spectroscopy [129,130]. Here, two spectrally distinct fluorophore tags are analyzed simultaneously as they move in and out of the focus. This technique is potentially a powerful tool to investigate protein–protein interactions in cells. However, thus far, FCS and related techniques have indicated their potential only with few live cell model applications [128,131,132]. Nonetheless FCS appears to be a very promising strategy to study protein concentrations and mobility, as well as intramolecular dynamics and binding kinetics within the lumen of mitochondria. For example, because FCS can monitor protein fluctuations of very rare proteins on short spatial distances it might be the method of choice to analyze the movement of proteins in and out of the cristae lumen. Similarly, it might be used to study the dynamic assembly of the large supercomplexes that reside in this organelle. With the nowadays commercially available FCS setups, it will be exciting to see how these techniques contribute to the analysis of protein dynamics within organelles.

12. FRET imaging microscopy

Yet another technique to investigate protein–protein interactions is fluorescence resonance energy transfer (FRET) imaging microscopy. Protein proximities (of proteins tagged with *different* fluorophores) in the sub-10 nm size regime can be probed by FRET imaging microscopy. The principle of FRET was formulated by Theodor Förster already in 1948 [133,134], but it was not until the advent of fluorescent proteins that FRET became a popular tool in live cell microscopy. FRET is a non-radiative transfer of energy from an excited fluorophore, the donor, to a second nearby fluorophore, the acceptor. The acceptor needs to have an excitation spectrum that overlaps with the donor emission. FRET is efficient at a fluorophore distance of 1–10 nm; hence FRET may be employed as a kind of ruler to determine whether two molecules are within this distance. A comprehensive overview on various FRET techniques is given by [135]. Descriptions of the practical implementation of FRET experiments are detailed in [136–139].

Several FP pairs with overlapping emission and excitation spectra are suitable for FRET; frequently used FRET pairs include CFP (cyan fluorescent protein) with YFP (yellow fluorescent protein) or GFP with RFP (red fluorescent protein) [140]. However, the early FPs had a number of spectroscopic limitations. For example, the enhanced cyan fluorescent protein (ECFP) exhibits a low quantum yield, a low extinction coefficient and a fluorescence lifetime that is best fit by a double exponential. With the directed development of novel FP variants [22,141–143], the number of potential FRET pairs has markedly increased so that for most applications a suitable FRET pair should be available.

In elegant cuvette experiments, the possibilities of FRET have been exploited by Prescott and colleagues to investigate the assembly and dimerization of the yeast F_1F_0–ATP synthase complex [144,145]. They monitored the dynamic changes in the spatial orientation of OSCP to subunit b, both of which are proteins of the synthase complex, tagged with BFP (blue fluorescent protein) and GFP, respectively. In an early FRET imaging microscopy study, the direct interaction of GFP-Bax with BFP-Bcl-2 in mitochondria has been demonstrated in live NIH3T3 cells [146]. In further applications of this strategy the caspase 8 mediated cleavage of Bid, which is a proapoptotic member of the Bcl-2 family was investigated [147]. To this end, functional YFP-Bid-CFP fusion proteins were expressed. By analyzing the FRET efficiency between the N-terminal YFP and the C-terminal CFP, the cleavage of YFP-Bid-CFP upon various stimuli was observed directly in live cells [147].

Currently, nonetheless, the mitochondrial functional problem that has been mostly tackled by using FRET, is arguably Ca^{2+} signaling, as expertly reviewed in [34,148,149]. Shortly after the introduction of GFP has a cellular probe, recombinant FP based Ca^{2+} sensors were developed [150,151]. These sensors, namely cameleon [150] and FIP-CB_{SM} [151] exhibited a similar design; both probes consist of two different FP variants that are linked by a Ca^{2+} responsive sequence element, i. e. the calmodulin (CaM)-binding peptide M13 fused to CaM [150], or only the M13 peptide [151]. They employ a similar strategy to convey Ca^{2+} concentrations: alterations of the FRET efficiency between the two different FP variants that are caused by the interaction of the Ca^{2+}-activated CaM with the M13 peptide are monitored. Several improved variants of these probes have later been developed [152–155]. In a series of studies, cameleons were used to monitor Ca^{2+} dynamics within mitochondria [156–160]. It should be noted, however, that also several other genetically encoded Ca^{2+} sensors have been developed, that do not rely on the analysis of the FRET efficiency and which might be advantageous for a given applications [34,149].

13. New techniques for high spatial resolution

In most cell types mitochondria have a tubular appearance. The mitochondrial tubules might be several μm long or connected to elaborated networks; however, their diameter is generally small, in budding yeast, for example, in the range of only about 350 nm [161]. Due to the spatially limited resolution power of light microscopy, these small diameters make it very challenging to investigate protein distributions within the volume of mitochondria using live cell light microscopy. With the currently available technologies, the cristae, for example, are too detailed to be recorded with light.

What is resolution anyway? Resolution is the minimal distance which a microscope can distinguish between two or more features of the same kind [162]. Therefore, resolution must not be confused with localization precision: It might easily be possible to localize a GFP-tagged protein complex with nanometer precision within an organelle, whereas a conventional widefield fluorescence microscope will fail to discriminate two GFP-tagged complexes that are 100 nm apart.

The wave nature of light imposes a seemingly fundamental limit on the resolving power of a microscope. According to Abbe, the resolution limitation is ultimately rooted in the phenomenon of diffraction [162]. Because of diffraction, focusing of light always results in a blurred spot [163], whose size determines the resolution. Thus, the highest achievable

resolution with objective lenses is ~180 nm in the imaging plane. The resolution along the optical axis is inescapably worse; even confocal or two photon fluorescence microscopes, which stand out by their ability to provide 3D images by optical sectioning, can only distinguish fluorescent objects if their axial distance is at least 500–800 nm.

The last decade has witnessed several new developments that have greatly improved the resolution of far field optical microscopy (for review see, [164–166]). Some of these, namely 4Pi microscopy have already been used to investigate mitochondria in vivo. Others are still emerging techniques, but arguably have the potential to image sub-mitochondrial protein or lipid distributions in live cells in the near future. Therefore, also these strategies are briefly discussed here.

14. Axial resolution improvement with two lenses

Conventional and confocal microscopy have a relatively poor axial resolution, because the focal spot of a single lens is at least 3- to 4-fold longer than it is wide [163,167]. An explanation for this focus asymmetry is that the focusing angle of a lens is not a full solid angle of 4π. If it was, the focal spot would be (virtually) round. Hence an evident strategy to decrease the axial spot size is to enlarge the focusing angle of the system by employing two opposing lenses with a common focus [168]. This concept of two opposing lenses has been successfully implemented in spot-scanning 4Pi confocal [169] and widefield I^5M microscopy [170]. Both techniques improve the axial resolution by enlarging the total aperture of the system. This is achieved by combining the spherical wavefronts of the two lenses by interference [171–173]. With these strategies, an up to 7-fold improved axial resolution could be obtained along the optical axis [173,174]. However, thus far, only 4Pi microscopy has demonstrated live cell imaging capabilities [161,175]. Multifocal multiphoton 4Pi microscopy (MMM-4Pi) is a 4Pi variant that uses an array of foci to scan the specimen. MMM-4Pi has been used to image the GFP labeled mitochondrial network of live budding yeast with an equilateral resolution of ~100 nm (Fig. 3) [161]. In this study, the morphological differences between the mitochondrial compartments of cells grown either on a fermentable carbon source (glucose) or on a non-fermentable carbon source (glycerol) were analyzed in detail. With 4Pi microscopy, the lateral resolution is essentially the same as with confocal microscopy. But whereas confocal microscopy fails to accurately determine the diameter of mitochondria, 4Pi microcopy is very well suited for this task: In 4Pi microscopy the interference of the spherical wavefronts of the two excitation beams results in a modulated focus [176]. Provided that a structure is thin enough (75–500 nm) and evenly labeled with a fluorophore, like mitochondria labeled with matrix targeted GFP, the modulation of the 4Pi focus depends on the diameter of this cellular structure. Hence the 4Pi microscope can be used to determine the thinness (or thickness) of mitochondria. Using this tool, it was demonstrated that the average mitochondrial tubule diameter in budding yeast changes from 339±5 nm to 360±4 nm, when the cells are shifted from a glucose containing medium to glycerol as a carbon source [161]. The observed shift was also accompanied by a 3.0±0.2-fold increase in the volume of the mitochondrial compartment, likely reflecting the increase of mitochondrial respiration when glycerol is the only carbon source.

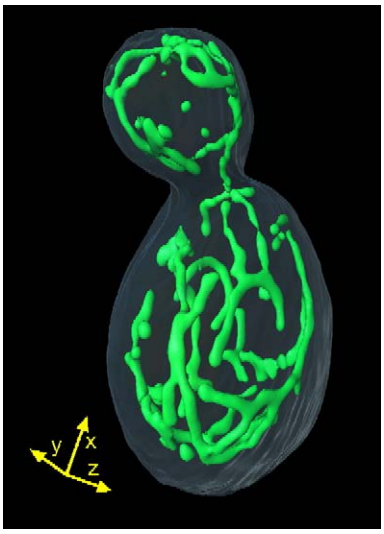

Fig. 3. 4Pi microscopy. Mitochondrial network of a live budding yeast cell recorded with an MMM-4Pi microscope at an equilateral resolution of ~100 nm. The mitochondrial matrix was labeled with GFP; displayed is a surface-rendered 3D-data stack. The cell wall has been stained with calcofluor white and displayed after interactive contour tracing. The length of each arrow corresponds to 1 μm. For details, see [161].

4Pi microscopy appears to be a mature technique, with a proven record of applications [161,175,177,178]. A commercial version of the 4Pi microscope is available (Leica Microsystems Heidelberg GmbH, Mannheim, Germany), so this technique is likely to experience a more widespread use in the future. Although 4Pi microscopy allows a 3D resolution in the 100 nm range, it is still ultimately limited by the diffraction barrier. Hence, it will not be possible to visualize detailed cristae morphologies using 4Pi microscopy, because they are well below the 100 nm limit. For this task, optical microscopy well below the diffraction barrier will be required.

15. Breaking the diffraction barrier

During the past decade, several physical concepts relying on *re*versible *s*aturable *o*ptica*l* *f*luorophore *t*ransitions (RESOLFT) have been developed by Stefan Hell and colleagues [179–182] that lay the theoretical fundamentals to eliminate the resolution-limiting effect of diffraction without eliminating diffraction. All members of the RESOLFT concept follow, in essence, a common principle to break Abbe's barrier. Strictly speaking, a focal intensity distribution with a zero-point in space effects a saturated molecular transition that – in one way or the other – inhibits the fluorescence of the dye. [164,165]. In these schemes the resolution is only determined by the photo-physical properties of the dye. Therefore there is no theoretical limit on the optical resolution, although in practice there will be limits like, for example, the photostability of the employed fluorophores.

Stimulated emission depletion (STED) microscopy was the first successfully employed RESOLFT scheme (Fig. 4). In stimulated emission, fluorophores that have just been excited to the fluorescence state S1 by an excitation pulse are immediately transferred by a second (STED) light pulse to the non-fluorescent ground state S_0 [179,183] (Fig. 4A). During this process, the fluorophore emits a photon with a wavelength corresponding to the STED-beam (hence, the term 'stimulated emission'), but no fluorescent photon. Loosely speaking, because of stimulated emission, the STED light pulse switches the already excited fluorophore off. This process is saturable, reversible and non-destructive. Importantly, STED microscopy requires not necessarily image processing and the signal intensity reflects the concentration of the fluorophores.

In its initial demonstration, STED microscopy has been realized as a point scanning system, whereby the excitation focus was a normal confocal spot and the STED focus resembled a doughnut, featuring a light intensity zero in the center [183]. Fig. 4B shows a typical experimental focal intensity distribution of the excitation spot (green), overlapping with a STED-spot (red) featuring a central intensity zero. Saturated depletion inhibits fluorescence everywhere except at the very center of the focal region. Using this experimental configuration, Klar et al. demonstrated the imaging of fluorescently labeled vacuolar membranes in live cells below the diffraction barrier, evidencing the live cell applicability of this approach [183]. In subsequent studies, STED and 4Pi microscopy have been synergistically combined to achieve a spatial resolution of ~50 nm in the imaging of the microtubule cytoskeleton of human cell lines [184]. Recently, STED microscopy has been used to study the clustering of synaptotagmin I, a protein resident in the membrane of synaptic vesicles [185]. Hence, since STED microscopy has already been employed for a number of applications, it appears likely that it is equally suited to study protein distributions within mitochondria.

Another example for a RESOLFT scheme is the saturation of the excited state itself (the fact that once the irradiation is intense enough to raise most fluorophores to the excited state, further intensity increases will not yield proportionate increases in the fluorescence emission) [186]. Saturation of the excited state combined with structured illumination has been used to create superior images of fluorescent beads spread on a cover slip with a 2D resolution of less than 50 nm [186,187]. Substantial computation, however, is required to obtain the final images. So far, this method has not been extended to 3D applications. Thus the coming years will show whether this method will be applicable for live cells and 3D imaging as well.

Very recently photoswitching of reversible switchable fluorescent proteins (RSFPs) has been demonstrated experimentally to be a mean to break the diffraction barrier [182,188]. With asFP595 and Dronpa, two RSFPs have been described so far [189,190]. The RSFP asFP595 may be transferred by green

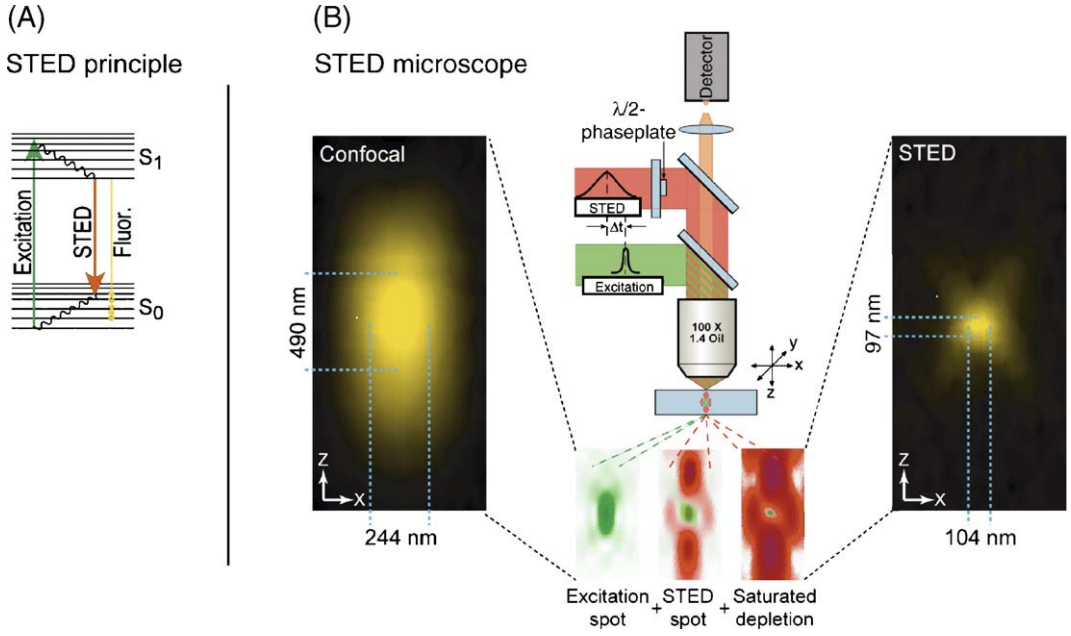

Fig. 4. STED-microscopy. (A) Molecules in the fluorescent state S_1 return to the ground state S_0 by spontaneous fluorescence emission. Return to S_0 may also be optically enforced through stimulated emission. To prevail over the spontaneous emission, stimulated emission depletion of the S_1 requires relatively intense light pulses with durations of a fraction of the S_1 lifetime. (B) Schematic of a point scanning STED-microscope. Excitation and STED are accomplished with synchronized laser pulses focused by a lens into the sample, sketched as green and red beams, respectively. Fluorescence is registered by a detector. Intensity distributions in the focus are shown at the bottom: The diffraction limited excitation spot (left) is overlapped with the doughnut shaped STED spot featuring a central intensity zero (center). Saturated depletion by the STED beam reduces the region of excited molecules (right) to the very zero-point, leaving a fluorescent spot of subdiffraction dimensions. The (measured) images on the left and right depict the confocal and the sub-diffraction-sized spot left by STED, respectively. Note the doubled lateral and 5-fold improved axial resolution of STED over confocal microscopy. The reduction in dimensions (x, y, z) yields an ultrasmall volume of subdiffraction size, here 0.67 attoliter, corresponding to an 18-fold reduction compared to its confocal counterpart. In spite of using diffraction limited beams, the concept of STED-fluorescence microscopy eliminates the resolution-limiting effect of diffraction. The spot size is not limited on principle grounds but by practical circumstances such as the quality of the zero and the saturation factor of depletion. Adapted from [165] with data from [183].

light from a nonfluorescent off- into a fluorescent on-state from which it reverts back eventually, but this transition can also be stimulated by gentle irradiation with blue light [189]. The protein may be driven through this 'on–off cycle' many times. Upon switching, asFP595 undergoes a trans- to cis-isomerization [191]. In the first proof-of-principle experiments, using purified asFP595 filled in artificially fabricated grooves, it was demonstrated that the saturable switching between the two states may be employed to surpass the diffraction barrier with very low light levels [188]. Currently, the photophysical properties of asFP595 are far from optimal, limiting its suitability for in vivo applications. Since asFP595 is a protein it is likely possible to improve asFP595's switching characteristics by mutagenesis. Because RSFPs are suited as genetically encodable tags like any other FP, they potentially open up a plethora of novel experimental strategies. Hence, reversible switchable proteins might be another very promising strategy for cellular imaging below the diffraction barrier.

Currently, STED microscopy is the most mature of these new techniques. But even STED microscopy is still a young approach. So it is likely to take some more years before these techniques will be available to a wider community.

16. Conclusions and perspectives

The imaging strategies described in this review have added vastly to our understanding of mitochondrial function. Since sophisticated imaging technology is now available in many laboratories, the contributions of live cell microscopy to the understanding of the cellular role of mitochondria will certainly continue.

Clearly, research in specialist' laboratories will persist to drive new innovations in imaging technologies. Fast and sensitive microscopes that allow a routine study of single molecules in live mitochondria would open up new research fields. Similarly, STED-4Pi microscopy already has provided an (axial) resolution of 50 nm in fixed cells [184]. Since published data imply the possibility of producing spherical focal volumes of 30 nm diameter [185,192,193], this value is more of a starting point than a limit. The availability of an optical microscope with an equilateral resolution of less than 50 nm may have a dramatic influence on our understanding of mitochondria, since it potentially would allow the study of sub-mitochondrial structure and dynamics in vivo.

Acknowledgements

I thank M. Andresen, S. Hell, J. Jethwa, S. Stoldt and C. Wurm for critically reading the manuscript. The microphotograph of Fig. 1B was kindly provided by A. Keppler and K. Johnsson. The continuous support by Stefan Hell is gratefully acknowledged. I wish to acknowledge financial support by the Deutsche Forschungsgemeinschaft (JA 1129/3).

References

[1] H.P. Hoffmann, C.J. Avers, Mitochondrion of yeast: Ultrastructural evidence for one giant, branched organelle per cell, Science 181 (1973) 749–751.
[2] J. Bereiter-Hahn, M. Voth, Dynamics of mitochondria in living cells: shape changes, dislocations, fusion, and fission of mitochondria, Microsc. Res. Tech. 27 (1994) 198–219.
[3] J. Nunnari, W.F. Marshall, A. Straight, A. Murray, J.W. Sedat, P. Walter, Mitochondrial transmission during mating in *Saccharomyces cerevisiae* is determined by mitochondrial fusion and fission and the intramitochondrial segregation of mitochondrial DNA, Mol. Biol. Cell 8 (1997) 1233–1242.
[4] H.M. Heath-Engel, G.C. Shore, Mitochondrial membrane dynamics, cristae remodelling and apoptosis, Biochim. Biophys. Acta 1763 (2006) 549–560.
[5] D.J. Stephens, V.J. Allan, Light microscopy techniques for live cell imaging, Science 300 (2003) 82–86.
[6] J. Pawley, Handbook of Biological Confocal Microscopy, Plemum Press, New York, 2006.
[7] J. Plasek, K. Sigler, Slow fluorescent indicators of membrane potential: a survey of different approaches to probe response analysis, J. Photochem. Photobiol., B 33 (1996) 101–124.
[8] J.A. Dykens, A.K. Stout, Assessment of mitochondrial membrane potential in situ using single potentiometric dyes and a novel fluorescence resonance energy transfer technique, Methods Cell Biol. 65 (2001) 285–309.
[9] M.R. Duchen, A. Surin, J. Jacobson, Imaging mitochondrial function in intact cells, Methods Enzymol. 361 (2003) 353–389.
[10] H. Rottenberg, S. Wu, Quantitative assay by flow cytometry of the mitochondrial membrane potential in intact cells, Biochim. Biophys. Acta 1404 (1998) 393–404.
[11] S. Salvioli, A. Ardizzoni, C. Franceschi, A. Cossarizza, JC-1, but not $DiOC_6(3)$ or rhodamine 123, is a reliable fluorescent probe to assess delta psi changes in intact cells: implications for studies on mitochondrial functionality during apoptosis, FEBS Lett. 411 (1997) 77–82.
[12] A. Mathur, Y. Hong, B.K. Kemp, A.A. Barrientos, J.D. Erusalimsky, Evaluation of fluorescent dyes for the detection of mitochondrial membrane potential changes in cultured cardiomyocytes, Cardiovasc. Res. 46 (2000) 126–138.
[13] R.P. Haugland, Handbook of Fluorescent Probes and Research Products, 9th ed.Molecular Probes, Inc., Eugene, OR, 2002.
[14] U. Erbrich, M. Septinus, A. Naujok, H.W. Zimmermann, Hydrophobic acridine dyes for fluorescence staining of mitochondria in living cells. 2. Comparison of staining of living and fixed HeLa-cells with NAO and DPPAO, Histochemistry 80 (1984) 385–398.
[15] B. Ehrenberg, V. Montana, M.D. Wei, J.P. Wuskell, L.M. Loew, Membrane potential can be determined in individual cells from the nernstian distribution of cationic dyes, Biophys. J. 53 (1988) 785–894.
[16] O. Shimomura, F.H. Johnson, Y. Saiga, Extraction, purification and properties of aequorin, a bioluminescent protein from the luminous hydromedusan, *Aequorea*, J. Cell. Comp. Physiol. 59 (1962) 223–239.
[17] F.H. Johnson, O. Shimomura, Y. Saiga, L.C. Gershman, G.T. Reynolds, J.R. Waters, Quantum efficiency of *Cypridina* luminescence, with a note on that of *Aequorea*, J. Cell. Comp. Physiol. 60 (1962) 85–103.
[18] D.C. Prasher, V.K. Eckenrode, W.W. Ward, F.G. Prendergast, M.J. Cormier, Primary structure of the *Aequorea victoria* green-fluorescent protein, Gene 111 (1992) 229–233.
[19] M. Chalfie, Y. Tu, G. Euskirchen, W.W. Ward, D.C. Prasher, Green fluorescent protein as a marker for gene expression, Science 263 (1994) 802–805.
[20] S. Inouye, F.I. Tsuji, *Aequorea* green fluorescent protein. Expression of the gene and fluorescence characteristics of the recombinant protein, FEBS Lett. 341 (1994) 277–280.
[21] R. Rizzuto, M. Brini, P. Pizzo, M. Murgia, T. Pozzan, Chimeric green fluorescent protein as a tool for visualizing subcellular organelles in living cells, Curr. Biol. 5 (1995) 635–642.
[22] N.C. Shaner, R.E. Campbell, P.A. Steinbach, B.N. Giepmans, A.E. Palmer, R.Y. Tsien, Improved monomeric red, orange and yellow fluorescent proteins derived from *Discosoma* sp. red fluorescent protein, Nat. Biotechnol. 22 (2004) 1567–1572.
[23] D.M. Chudakov, S. Lukyanov, K.A. Lukyanov, Fluorescent proteins as a toolkit for in vivo imaging, Trends Biotechnol. 23 (2005) 605–613.

[24] P.D. Gavin, M. Prescott, S.E. Luff, R.J. Devenish, Cross-linking ATP synthase complexes in vivo eliminates mitochondrial cristae, J. Cell Sci. 117 (2004) 2333–2343.
[25] R.E. Campbell, O. Tour, A.E. Palmer, P.A. Steinbach, G.S. Baird, D.A. Zacharias, R.Y. Tsien, A monomeric red fluorescent protein, Proc. Natl. Acad. Sci. U. S. A. 99 (2002) 7877–7882.
[26] N.C. Shaner, P.A. Steinbach, R.Y. Tsien, A guide to choosing fluorescent proteins, Nat. Methods 2 (2005) 905–909.
[27] A.M. Porcelli, P. Pinton, E.K. Ainscow, A. Chiesa, M. Rugolo, G.A. Rutter, R. Rizzuto, Targeting of reporter molecules to mitochondria to measure calcium, ATP, and pH, Methods Cell Biol. 65 (2001) 353–380.
[28] J. Zhang, R.E. Campbell, A.Y. Ting, R.Y. Tsien, Creating new fluorescent probes for cell biology, Nat. Rev., Mol. Cell Biol. 3 (2002) 906–918.
[29] M. Kneen, J. Farinas, Y. Li, A.S. Verkman, Green fluorescent protein as a noninvasive intracellular pH indicator, Biophys. J. 74 (1998) 1591–1599.
[30] J. Llopis, J.M. McCaffery, A. Miyawaki, M.G. Farquhar, R.Y. Tsien, Measurement of cytosolic, mitochondrial, and Golgi pH in single living cells with green fluorescent proteins, Proc. Natl. Acad. Sci. U. S. A. 95 (1998) 6803–6808.
[31] M.F. Abad, G. Di Benedetto, P.J. Magalhaes, L. Filippin, T. Pozzan, Mitochondrial pH monitored by a new engineered green fluorescent protein mutant, J. Biol. Chem. 279 (2004) 11521–11529.
[32] A.M. Porcelli, A. Ghelli, C. Zanna, P. Pinton, R. Rizzuto, M. Rugolo, pH difference across the outer mitochondrial membrane measured with a green fluorescent protein mutant, Biochem. Biophys. Res. Commun. 326 (2005) 799–804.
[33] G.T. Hanson, R. Aggeler, D. Oglesbee, M. Cannon, R.A. Capaldi, R.Y. Tsien, S.J. Remington, Investigating mitochondrial redox potential with redox-sensitive green fluorescent protein indicators, J. Biol. Chem. 279 (2004) 13044–13053.
[34] R. Rudolf, M. Mongillo, R. Rizzuto, T. Pozzan, Looking forward to seeing calcium, Nat. Rev., Mol. Cell Biol. 4 (2003) 579–586.
[35] W.K. Huh, J.V. Falvo, L.C. Gerke, A.S. Carroll, R.W. Howson, J.S. Weissman, E.K. O'Shea, Global analysis of protein localization in budding yeast, Nature 425 (2003) 686–691.
[36] A. Sickmann, J. Reinders, Y. Wagner, C. Joppich, R. Zahedi, H.E. Meyer, B. Schonfisch, I. Perschil, A. Chacinska, B. Guiard, P. Rehling, N. Pfanner, C. Meisinger, The proteome of *Saccharomyces cerevisiae* mitochondria, Proc. Natl. Acad. Sci. U. S. A. 100 (2003) 13207–13212.
[37] H. Prokisch, C. Scharfe, D.G. Camp, W. Xiao, L. David, C. Andreoli, M.E. Monroe, R.J. Moore, M.A. Gritsenko, C. Kozany, K.K. Hixson, H.M. Mottaz, H. Zischka, M. Ueffing, Z.S. Herman, R.W. Davis, T. Meitinger, P.J. Oefner, R.D. Smith, L.M. Steinmetz, Integrative analysis of the mitochondrial proteome in yeast, PLoS Biol. 2 (2004) e160.
[38] A.S. Reichert, W. Neupert, Mitochondriomics or what makes us breathe, Trends Genet. 20 (2004) 555–562.
[39] R.P. Zahedi, A. Sickmann, A.M. Boehm, C. Winkler, N. Zufall, B. Schonfisch, B. Guiard, N. Pfanner, C. Meisinger, Proteomic analysis of the yeast mitochondrial outer membrane reveals accumulation of a subclass of preproteins, Mol. Biol. Cell 17 (2006) 1436–1450.
[40] N. Johnsson, K. Johnsson, A fusion of disciplines: chemical approaches to exploit fusion proteins for functional genomics, ChemBioChem 4 (2003) 803–810.
[41] I. Chen, A.Y. Ting, Site-specific labeling of proteins with small molecules in live cells, Curr. Opin. Biotechnol. 16 (2005) 35–40.
[42] T. Gronemeyer, G. Godin, K. Johnsson, Adding value to fusion proteins through covalent labelling, Curr. Opin. Biotechnol. 16 (2005) 453–458.
[43] L.W. Miller, V.W. Cornish, Selective chemical labeling of proteins in living cells, Curr. Opin. Chem. Biol. 9 (2005) 56–61.
[44] J.A. Prescher, C.R. Bertozzi, Chemistry in living systems, Nat. Chem. Biol. 1 (2005) 13–21.
[45] B.A. Griffin, S.R. Adams, R.Y. Tsien, Specific covalent labeling of recombinant protein molecules inside live cells, Science 281 (1998) 269–672.
[46] G. Gaietta, T.J. Deerinck, S.R. Adams, J. Bouwer, O. Tour, D.W. Laird, G.E. Sosinsky, R.Y. Tsien, M.H. Ellisman, Multicolor and electron microscopic imaging of connexin trafficking, Science 296 (2002) 503–507.
[47] R.G. Panchal, G. Ruthel, T.A. Kenny, G.H. Kallstrom, D. Lane, S.S. Badie, L. Li, S. Bavari, M.J. Aman, In vivo oligomerization and raft localization of Ebola virus protein vp40 during vesicular budding, Proc. Natl. Acad. Sci. U. S. A. 100 (2003) 15936–15941.
[48] M. Andresen, R. Schmitz-Salue, S. Jakobs, Short tetracysteine tags to beta-tubulin demonstrate the significance of small labels for live cell imaging, Mol. Biol. Cell 15 (2004) 5616–5622.
[49] C. Hoffmann, G. Gaietta, M. Bunemann, S.R. Adams, S. Oberdorff-Maass, B. Behr, J.P. Vilardaga, R.Y. Tsien, M.H. Ellisman, M.J. Lohse, A FlAsH-based FRET approach to determine g protein-coupled receptor activation in living cells, Nat. Methods 2 (2005) 171–176.
[50] S.R. Adams, R.E. Campbell, L.A. Gross, B.R. Martin, G.K. Walkup, Y. Yao, J. Llopis, R.Y. Tsien, New biarsenical ligands and tetracysteine motifs for protein labeling in vitro and in vivo: synthesis and biological applications, J. Am. Chem. Soc. 124 (2002) 6063–6076.
[51] K. Stroffekova, C. Proenza, K.G. Beam, The protein-labeling reagent FlAsH-EDT_2 binds not only to CCXXCC motifs but also non-specifically to endogenous cysteine-rich proteins, Pflugers Arch. 442 (2001) 859–866.
[52] B.R. Martin, B.N. Giepmans, S.R. Adams, R.Y. Tsien, Mammalian cell-based optimization of the biarsenical-binding tetracysteine motif for improved fluorescence and affinity, Nat. Biotechnol. 23 (2005) 1308–1314.
[53] A. Keppler, S. Gendreizig, T. Gronemeyer, H. Pick, H. Vogel, K. Johnsson, A general method for the covalent labeling of fusion proteins with small molecules in vivo, Nat. Biotechnol. 21 (2003) 86–89.
[54] A. Juillerat, T. Gronemeyer, A. Keppler, S. Gendreizig, H. Pick, H. Vogel, K. Johnsson, Directed evolution of o6-alkylguanine-DNA alkyltransferase for efficient labeling of fusion proteins with small molecules in vivo, Chem. Biol. 10 (2003) 313–317.
[55] A. Keppler, H. Pick, C. Arrivoli, H. Vogel, K. Johnsson, Labeling of fusion proteins with synthetic fluorophores in live cells, Proc. Natl. Acad. Sci. U. S. A. 101 (2004) 9955–9959.
[56] A. Regoes, A.B. Hehl, Snap-tag mediated live cell labeling as an alternative to GFP in anaerobic organisms, BioTechniques 39 (2005) 809–810.
[57] R. Rizzuto, M. Brini, F. De Giorgi, R. Rossi, R. Heim, R.Y. Tsien, T. Pozzan, Double labelling of subcellular structures with organelle-targeted GFP mutants in vivo, Curr. Biol. 6 (1996) 183–188.
[58] T.J. Collins, M.J. Berridge, P. Lipp, M.D. Bootman, Mitochondria are morphologically and functionally heterogeneous within cells, EMBO J. 21 (2002) 1616–1627.
[59] M. Karbowski, R.J. Youle, Dynamics of mitochondrial morphology in healthy cells and during apoptosis, Cell Death Differ. 10 (2003) 870–880.
[60] D.C. Logan, C.J. Leaver, Mitochondria-targeted GFP highlights the heterogeneity of mitochondrial shape, size and movement within living plant cells, J. Exp. Bot. 51 (2000) 865–871.
[61] K. VanGestel, R.H. Kohler, J.P. Verbelen, Plant mitochondria move on F-actin, but their positioning in the cortical cytoplasm depends on both F-actin and microtubules, J. Exp. Bot. 53 (2002) 659–667.
[62] S. Jakobs, N. Martini, A.C. Schauss, A. Egner, B. Westermann, S.W. Hell, Spatial and temporal dynamics of budding yeast mitochondria lacking the division component Fis1p, J. Cell Sci. 116 (2003) 2005–2014.
[63] K.L. Fehrenbacher, H.C. Yang, A.C. Gay, T.M. Huckaba, L.A. Pon, Live cell imaging of mitochondrial movement along actin cables in budding yeast, Curr. Biol. 14 (2004) 1996–2004.
[64] S.W. Gorsich, J.M. Shaw, Importance of mitochondrial dynamics during meiosis and sporulation, Mol. Biol. Cell 15 (2004) 4369–4381.
[65] E. Bossy-Wetzel, M.J. Barsoum, A. Godzik, R. Schwarzenbacher, S.A. Lipton, Mitochondrial fission in apoptosis, neurodegeneration and aging, Curr. Opin. Cell Biol. 15 (2003) 706–716.
[66] J.L. Perfettini, T. Roumier, G. Kroemer, Mitochondrial fusion and fission in the control of apoptosis, Trends Cell Biol. 15 (2005) 179–183.
[67] C. Thomas, P. DeVries, J. Hardin, J. White, Four-dimensional imaging: computer visualization of 3D movements in living specimens, Science 273 (1996) 603–607.

[68] A.T. Hammond, B.S. Glick, Raising the speed limits for 4D fluorescence microscopy, Traffic 1 (2000) 935–940.
[69] D. Gerlich, J. Ellenberg, 4D imaging to assay complex dynamics in live specimens, Nat. Cell Biol. (2003) S14–S19.
[70] G.S. Harms, L. Cognet, P.H. Lommerse, G.A. Blab, T. Schmidt, Autofluorescent proteins in single-molecule research: applications to live cell imaging microscopy, Biophys. J. 80 (2001) 2396–2408.
[71] R. Rizzuto, A.W. Simpson, M. Brini, T. Pozzan, Rapid changes of mitochondrial Ca^{2+} revealed by specifically targeted recombinant aequorin, Nature 358 (1992) 325–327.
[72] B. Westermann, W. Neupert, Mitochondria-targeted green fluorescent proteins: convenient tools for the study of organelle biogenesis in *Saccharomyces cerevisiae*, Yeast 16 (2000) 1421–1427.
[73] A.D. Mozdy, J.M. McCaffery, J.M. Shaw, Dnm1p GTPase-mediated mitochondrial fission is a multi-step process requiring the novel integral membrane component Fis1p, J. Cell Biol. 151 (2000) 367–379.
[74] H. Sesaki, R.E. Jensen, Ugo1 encodes an outer membrane protein required for mitochondrial fusion, J. Cell Biol. 152 (2001) 1123–1134.
[75] J. Nunnari, E.D. Wong, S. Meeusen, J.A. Wagner, Studying the behavior of mitochondria, Methods Enzymol. 351 (2002) 381–393.
[76] M. Messerschmitt, S. Jakobs, F. Vogel, S. Fritz, K.S. Dimmer, W. Neupert, B. Westermann, The inner membrane protein Mdm33 controls mitochondrial morphology in yeast, J. Cell Biol. 160 (2003) 553–564.
[77] E.D. Wong, J.A. Wagner, S.V. Scott, V. Okreglak, T.J. Holewinske, A. Cassidy-Stone, J. Nunnari, The intramitochondrial dynamin-related GTPase, Mgm1p, is a component of a protein complex that mediates mitochondrial fusion, J. Cell Biol. 160 (2003) 303–311.
[78] H. Sesaki, R.E. Jensen, Ugo1p links the Fzo1p and Mgm1p GTPases for mitochondrial fusion, J. Biol. Chem. 279 (2004) 28298–28303.
[79] K.S. Dimmer, S. Jakobs, F. Vogel, K. Altmann, B. Westermann, Mdm31 and Mdm32 are inner membrane proteins required for maintenance of mitochondrial shape and stability of mitochondrial DNA nucleoids in yeast, J. Cell Biol. 168 (2005) 103–115.
[80] M.B. Sheahan, D.W. McCurdy, R.J. Rose, Mitochondria as a connected population: ensuring continuity of the mitochondrial genome during plant cell dedifferentiation through massive mitochondrial fusion, Plant J. 44 (2005) 744–755.
[81] F. Legros, A. Lombes, P. Frachon, M. Rojo, Mitochondrial fusion in human cells is efficient, requires the inner membrane potential, and is mediated by mitofusins, Mol. Biol. Cell 13 (2002) 4343–4354.
[82] N. Ishihara, A. Jofuku, Y. Eura, K. Mihara, Regulation of mitochondrial morphology by membrane potential, and Drp1-dependent division and Fzo1-dependent fusion reaction in mammalian cells, Biochem. Biophys. Res. Commun. 301 (2003) 891–898.
[83] H. Chen, S.A. Detmer, A.J. Ewald, E.E. Griffin, S.E. Fraser, D.C. Chan, Mitofusins Mfn1 and Mfn2 coordinately regulate mitochondrial fusion and are essential for embryonic development, J. Cell Biol. 160 (2003) 189–200.
[84] Y. Mattenberger, D.I. James, J.C. Martinou, Fusion of mitochondria in mammalian cells is dependent on the mitochondrial inner membrane potential and independent of microtubules or actin, FEBS Lett. 538 (2003) 53–59.
[85] F. Malka, O. Guillery, C. Cifuentes-Diaz, E. Guillou, P. Belenguer, A. Lombes, M. Rojo, Separate fusion of outer and inner mitochondrial membranes, EMBO Rep. 6 (2005) 853–859.
[86] I. Ghosh, A.D. Hamilton, L. Regan, Antiparallel leucine zipper-directed protein reassembly: application to the green fluorescent protein, J. Am. Chem. Soc. 122 (2000) 5658–5659.
[87] C.D. Hu, Y. Chinenov, T.K. Kerppola, Visualization of interactions among bZIP and Rel family proteins in living cells using bimolecular fluorescence complementation, Mol. Cell 9 (2002) 789–798.
[88] T.J. Magliery, C.G. Wilson, W. Pan, D. Mishler, I. Ghosh, A.D. Hamilton, L. Regan, Detecting protein–protein interactions with a green fluorescent protein fragment reassembly trap: scope and mechanism, J. Am. Chem. Soc. 127 (2005) 146–157.
[89] C.G. Wilson, T.J. Magliery, L. Regan, Detecting protein–protein interactions with GFP-fragment reassembly, Nat. Methods 1 (2004) 255–562.
[90] C.D. Hu, T.K. Kerppola, Simultaneous visualization of multiple protein interactions in living cells using multicolor fluorescence complementation analysis, Nat. Biotechnol. 21 (2003) 539–545.
[91] B. Nyfeler, S.W. Michnick, H.P. Hauri, Capturing protein interactions in the secretory pathway of living cells, Proc. Natl. Acad. Sci. U. S. A. 102 (2005) 6350–6355.
[92] Y.J. Shyu, H. Liu, X. Deng, C.D. Hu, Identification of new fluorescent protein fragments for bimolecular fluorescence complementation analysis under physiological conditions, BioTechniques 40 (2006) 61–66.
[93] S. Cabantous, T.C. Terwilliger, G.S. Waldo, Protein tagging and detection with engineered self-assembling fragments of green fluorescent protein, Nat. Biotechnol. 23 (2005) 102–107.
[94] R. Peters, J. Peters, K.H. Tews, W. Bahr, A microfluorimetric study of translational diffusion in erythrocyte membranes, Biochim. Biophys. Acta 367 (1974) 282–294.
[95] D. Axelrod, D.E. Koppel, J. Schlessinger, E. Elson, W.W. Webb, Mobility measurement by analysis of fluorescence photobleaching recovery kinetics, Biophys. J. 16 (1976) 1055–1069.
[96] M. Edidin, Y. Zagyansky, T.J. Lardner, Measurement of membrane protein lateral diffusion in single cells, Science 191 (1976) 466–468.
[97] K. Jacobson, E.S. Wu, G. Poste, Measurement of the translational mobility of concanavalin A in glycerol-saline solutions and on the cell surface by fluorescence recovery after photobleaching, Biochim. Biophys. Acta 433 (1976) 215–222.
[98] J. Schlessinger, D.E. Koppel, D. Axelrod, K. Jacobson, W.W. Webb, E.L. Elson, Lateral transport on cell membranes: mobility of concanavalin A receptors on myoblasts, Proc. Natl. Acad. Sci. U. S. A. 73 (1976) 2409–2413.
[99] E.A.J. Reits, J.J. Neefjes, From fixed to FRAP: measuring protein mobility and activity in living cells, Nat. Cell Biol. 3 (2001) E145–E147.
[100] J. Lippincott-Schwartz, N. Altan-Bonnet, G.H. Patterson, Photobleaching and photoactivation: following protein dynamics in living cells, Nat. Cell Biol. (2003) S7–S14.
[101] M. Köster, T. Frahm, H. Hauser, Nucleocytoplasmic shuttling revealed by FRAP and FLIP technologies, Curr. Opin. Biotechnol. 16 (2005) 28–34.
[102] B.L. Sprague, J.G. McNally, FRAP analysis of binding: proper and fitting, Trends Cell Biol. 15 (2005) 84–91.
[103] M. Dundr, U. Hoffmann-Rohrer, Q. Hu, I. Grummt, L.I. Rothblum, R.D. Phair, T. Misteli, A kinetic framework for a mammalian RNA polymerase in vivo, Science 298 (2002) 1623–1626.
[104] H. Mogami, K. Nakano, A.V. Tepikin, O.H. Petersen, Ca^{2+} flow via tunnels in polarized cells: recharging of apical Ca^{2+} stores by focal Ca^{2+} entry through basal membrane patch, Cell 88 (1997) 49–55.
[105] V.P. Skulachev, Mitochondrial filaments and clusters as intracellular power-transmitting cables, Trends Biochem. Sci. 26 (2001) 23–29.
[106] R. Rizzuto, P. Pinton, W. Carrington, F.S. Fay, K.E. Fogarty, L.M. Lifshitz, R.A. Tuft, T. Pozzan, Close contacts with the endoplasmic reticulum as determinants of mitochondrial Ca^{2+} responses, Science 280 (1998) 1763–1766.
[107] T.J. Collins, M.D. Bootman, Mitochondria are morphologically heterogeneous within cells, J. Exp. Biol. 206 (2003) 1993–2000.
[108] M.K. Park, M.C. Ashby, G. Erdemli, O.H. Petersen, A.V. Tepikin, Perinuclear, perigranular and sub-plasmalemmal mitochondria have distinct functions in the regulation of cellular calcium transport, EMBO J. 20 (2001) 1374–1863.
[109] A. Partikian, B. Olveczky, R. Swaminathan, Y.X. Li, A.S. Verkman, Rapid diffusion of green fluorescent protein in the mitochondrial matrix, J. Cell Biol. 140 (1998) 821–829.
[110] B.P. Olveczky, A.S. Verkman, Monte carlo analysis of obstructed diffusion in three dimensions—Application to molecular diffusion in organelles, Biophys. J. 74 (1998) 2722–2730.
[111] C.R. Hackenbrock, Chemical and physical fixation of isolated mitochondria in low-energy and high-energy states, Proc. Natl. Acad. Sci. U. S. A. 61 (1968) 598–605.
[112] P.A. Srere, The infrastructure of the mitochondrial matrix, Trends Biochem. Sci. 5 (1980) 120–121.
[113] P.M. Haggie, A.S. Verkman, Diffusion of tricarboxylic acid cycle enzymes in the mitochondrial matrix in vivo. Evidence for restricted

mobility of a multienzyme complex, J. Biol. Chem. 277 (2002) 40782–40788.
[114] K.A. Lukyanov, D.M. Chudakov, S. Lukyanov, V.V. Verkhusha, Innovation: photoactivatable fluorescent proteins, Nat. Rev., Mol. Cell Biol. 6 (2005) 885–891.
[115] M.B. Elowitz, M.G. Surette, P.E. Wolf, J. Stock, S. Leibler, Photoactivation turns green fluorescent protein red, Curr. Biol. 7 (1997) 809–812.
[116] K.E. Sawin, P. Nurse, Photoactivation of green fluorescent protein, Curr. Biol. 7 (1997) R606–R607.
[117] S. Jakobs, A.C. Schauss, S.W. Hell, Photoconversion of matrix targeted GFP enables analysis of continuity and intermixing of the mitochondrial lumen, FEBS Lett. 554 (2003) 194–200.
[118] S. Arimura, J. Yamamoto, G.P. Aida, M. Nakazono, N. Tsutsumi, Frequent fusion and fission of plant mitochondria with unequal nucleoid distribution, Proc. Natl. Acad. Sci. U. S. A. 101 (2004) 7805–7808.
[119] M. Karbowski, D. Arnoult, H. Chen, D.C. Chan, C.L. Smith, R.J. Youle, Quantitation of mitochondrial dynamics by photolabeling of individual organelles shows that mitochondrial fusion is blocked during the bax activation phase of apoptosis, J. Cell Biol. 164 (2004) 493–499.
[120] G.H. Patterson, J. Lippincott-Schwartz, A photoactivatable GFP for selective photolabeling of proteins and cells, Science 297 (2002) 1873–1877.
[121] R. Ando, H. Hama, M. Yamamoto-Hino, H. Mizuno, A. Miyawaki, An optical marker based on the UV-induced green-to-red photoconversion of a fluorescent protein, Proc. Natl. Acad. Sci. U. S. A. 99 (2002) 12651–12656.
[122] D. Magde, E. Elson, W.W. Webb, Thermodynamic fluctuations in a reacting system: measurement by fluorescence correlation spectroscopy, Phys. Rev. Lett. 29 (1972) 705–708.
[123] M. Eigen, R. Rigler, Sorting single molecules: application to diagnostics and evolutionary biotechnology, Proc. Natl. Acad. Sci. U. S. A. 91 (1994) 5740–5747.
[124] R. Rigler, E.S. Elson (Eds.), Fluorescence correlation spectroscopy. Theory and applications, vol. 65, Springer-Verlag, Berlin, 2001.
[125] R. Brock, T.M. Jovin, Fluorescence correlation microscopy (FCM): Fluorescence correlation spectroscopy (FCS) in cell biology, in: Springer series in chemical physics, Fluorescence Correlation Spectroscopy: Theory and Applications, vol. 65, Springer-Verlag, Berlin, 2001, pp. 132–161.
[126] S.T. Hess, S. Huang, A.A. Heikal, W.W. Webb, Biological and chemical applications of fluorescence correlation spectroscopy: A review, Biochemistry 41 (2002) 697–705.
[127] J.D. Muller, Y. Chen, E. Gratton, Fluorescence correlation spectroscopy, Methods Enzymol 361 (2003) 69–92.
[128] T. Kohl, P. Schwille, Fluorescence correlation spectroscopy with autofluorescent proteins, Adv. Biochem. Eng. Biotechnol. 95 (2005) 107–142.
[129] P. Schwille, F.J. Meyer-Almes, R. Rigler, Dual-color fluorescence cross-correlation spectroscopy for multicomponent diffusional analysis in solution, Biophys. J. 72 (1997) 1878–1886.
[130] K.G. Heinze, A. Koltermann, P. Schwille, Simultaneous two-photon excitation of distinct labels for dual-color fluorescence crosscorrelation analysis, Proc. Natl. Acad. Sci. U. S. A. 97 (2000) 10377–10382.
[131] M.A. Digman, C.M. Brown, P. Sengupta, P.W. Wiseman, A.R. Horwitz, E. Gratton, Measuring fast dynamics in solutions and cells with a laser scanning microscope, Biophys. J. 89 (2005) 1317–1327.
[132] D.R. Larson, J.A. Gosse, D.A. Holowka, B.A. Baird, W.W. Webb, Temporally resolved interactions between antigen-stimulated IgE receptors and Lyn kinase on living cells, J. Cell Biol. 171 (2005) 527–536.
[133] T. Förster, Intermolecular energy migration and fluorescence, Ann. Phys. (Leipzig) 2 (1948) 55–75.
[134] J.R. Lakowicz, Principles of Fluorescence Spectroscopy, 2nd ed.Plenum Press, New York, 1999.
[135] E.A. Jares-Erijman, T.M. Jovin, FRET imaging, Nat. Biotechnol. 21 (2003) 1387–1395.
[136] P. Wu, L. Brand, Resonance energy transfer: methods and applications, Anal. Biochem. 218 (1994) 1–13.
[137] A.K. Kenworthy, Imaging protein–protein interactions using fluorescence resonance energy transfer microscopy, Methods 24 (2001) 289–296.
[138] K. Truong, M. Ikura, The use of FRET imaging microscopy to detect protein–protein interactions and protein conformational changes in vivo, Curr. Opin. Struct. Biol. 11 (2001) 573–578.
[139] V.E. Centonze, M. Sun, A. Masuda, H. Gerritsen, B. Herman, Fluorescence resonance energy transfer imaging microscopy, Methods Enzymol. 360 (2003) 542–560.
[140] H. Mizuno, A. Sawano, P. Eli, H. Hama, A. Miyawaki, Red fluorescent protein from *Discosoma* as a fusion tag and a partner for fluorescence resonance energy transfer, Biochemistry 40 (2001) 2502–2510.
[141] S. Karasawa, T. Araki, T. Nagai, H. Mizuno, A. Miyawaki, Cyan-emitting and orange-emitting fluorescent proteins as a donor/acceptor pair for fluorescence resonance energy transfer, Biochem. J. 381 (2004) 307–312.
[142] M.A. Rizzo, G.H. Springer, B. Granada, D.W. Piston, An improved cyan fluorescent protein variant useful for FRET, Nat. Biotechnol. 22 (2004) 445–449.
[143] A.W. Nguyen, P.S. Daugherty, Evolutionary optimization of fluorescent proteins for intracellular FRET, Nat. Biotechnol. 23 (2005) 355–360.
[144] P.D. Gavin, R.J. Devenish, M. Prescott, FRET reveals changes in the F_1-stator stalk interaction during activity of F_1F_0-ATP synthase, Biochim. Biophys. Acta 1607 (2003) 167–179.
[145] P.D. Gavin, M. Prescott, R.J. Devenish, F_1F_0-ATP synthase complex interactions in vivo can occur in the absence of the dimer specific subunit e, J. Bioenerg. Biomembr. 37 (2005) 55–66.
[146] N.P. Mahajan, K. Linder, G. Berry, G.W. Gordon, R. Heim, B. Herman, Bcl-2 and Bax interactions in mitochondria probed with green fluorescent protein and fluorescence resonance energy transfer, Nat. Biotechnol. 16 (1998) 547–552.
[147] R. Onuki, A. Nagasaki, H. Kawasaki, T. Baba, T.Q. Uyeda, K. Taira, Confirmation by FRET in individual living cells of the absence of significant amyloid beta-mediated caspase 8 activation, Proc. Natl. Acad. Sci. U. S. A. 99 (2002) 14716–14721.
[148] A. Miyawaki, Visualization of the spatial and temporal dynamics of intracellular signaling, Dev. Cell 4 (2003) 295–305.
[149] N. Demaurex, Calcium measurements in organelles with Ca^{2+}-sensitive fluorescent proteins, Cell Calcium 38 (2005) 213–322.
[150] A. Miyawaki, J. Llopis, R. Heim, J.M. McCaffery, J.A. Adams, M. Ikura, R.Y. Tsien, Fluorescent indicators for Ca^{2+} based on green fluorescent proteins and calmodulin, Nature 388 (1997) 882–887.
[151] V.A. Romoser, P.M. Hinkle, A. Persechini, Detection in living cells of Ca^{2+}-dependent changes in the fluorescence emission of an indicator composed of two green fluorescent protein variants linked by a calmodulin-binding sequence. A new class of fluorescent indicators, J. Biol. Chem. 272 (1997) 13270–13274.
[152] A. Miyawaki, O. Griesbeck, R. Heim, R.Y. Tsien, Dynamic and quantitative Ca^{2+} measurements using improved cameleons, Proc. Natl. Acad. Sci. U. S. A. 96 (1999) 2135–2140.
[153] K. Truong, A. Sawano, H. Mizuno, H. Hama, K.I. Tong, T.K. Mal, A. Miyawaki, M. Ikura, FRET-based in vivo Ca^{2+} imaging by a new calmodulin-GFP fusion molecule, Nat. Struct. Biol. 8 (2001) 1069–1073.
[154] N. Heim, O. Griesbeck, Genetically encoded indicators of cellular calcium dynamics based on troponin C and green fluorescent protein, J. Biol. Chem. 279 (2004) 14280–14286.
[155] L. Filippin, M.C. Abad, S. Gastaldello, P.J. Magalhaes, D. Sandona, T. Pozzan, Improved strategies for the delivery of GFP-based Ca^{2+} sensors into the mitochondrial matrix, Cell Calcium 37 (2005) 129–136.
[156] M. Jaconi, C. Bony, S.M. Richards, A. Terzic, S. Arnaudeau, G. Vassort, M. Puceat, Inositol 1,4,5-trisphosphate directs $Ca^{(2+)}$ flow between mitochondria and the endoplasmic/sarcoplasmic reticulum: a role in regulating cardiac autonomic $Ca^{(2+)}$ spiking, Mol. Biol. Cell 11 (2000) 1845–1858.
[157] S. Arnaudeau, W.L. Kelley, J.V. Walsh Jr., N. Demaurex, Mitochondria recycle $Ca^{(2+)}$ to the endoplasmic reticulum and prevent the depletion of neighboring endoplasmic reticulum regions, J. Biol. Chem. 276 (2001) 29430–29439.

[158] S. Arnaudeau, M. Frieden, K. Nakamura, C. Castelbou, M. Michalak, N. Demaurex, Calreticulin differentially modulates calcium uptake and release in the endoplasmic reticulum and mitochondria, J. Biol. Chem. 277 (2002) 46696–46705.
[159] R. Malli, M. Frieden, K. Osibow, W.F. Graier, Mitochondria efficiently buffer subplasmalemmal Ca^{2+} elevation during agonist stimulation, J. Biol. Chem. 278 (2003) 10807–10815.
[160] R. Rudolf, M. Mongillo, P.J. Magalhaes, T. Pozzan, In vivo monitoring of $Ca^{(2+)}$ uptake into mitochondria of mouse skeletal muscle during contraction, J. Cell Biol. 166 (2004) 527–536.
[161] A. Egner, S. Jakobs, S.W. Hell, Fast 100-nm resolution three-dimensional microscope reveals structural plasticity of mitochondria in live yeast, Proc. Natl. Acad. Sci. U. S. A. 99 (2002) 3370–3375.
[162] E. Abbe, Beiträge zur Theorie des Mikroskops und der mikroskopischen Wahrnehmung, Arch. Mikrosk. Anat. 9 (1873) 413–420.
[163] M. Born, E. Wolf, Principles of Optics, 7th ed. Cambridge Univ. Press, Cambridge, 2002.
[164] S.W. Hell, Toward fluorescence nanoscopy, Nat. Biotechnol. 21 (2003) 1347–1355.
[165] S.W. Hell, M. Dyba, S. Jakobs, Concepts for nanoscale resolution in fluorescence microscopy, Curr. Opin. Neurobiol. 14 (2004) 599–609.
[166] Y. Garini, B.J. Vermolen, I.T. Young, From micro to nano: recent advances in high-resolution microscopy, Curr. Opin. Biotechnol. 16 (2005) 3–12.
[167] T. Wilson, C.J.R. Sheppard, Theory and practice of scanning optical microscopy, Academic Press, New York, 1984.
[168] S. Hell, E.H.K. Stelzer, Properties of a 4Pi-confocal fluorescence microscope, J. Opt. Soc. Am. A 9 (1992) 2159–2166.
[169] S.W. Hell, E.H.K. Stelzer, Fundamental improvement of resolution with a 4Pi-confocal fluorescence microscope using two-photon excitation, Opt. Commun. 93 (1992) 277–282.
[170] M.G.L. Gustafsson, D.A. Agard, J.W. Sedat, Sevenfold improvement of axial resolution in 3D widefield microscopy using two objective lenses, Proc. Soc. Photo-Opt. Instrum. Eng. 2412 (1995) 147–156.
[171] M. Schrader, S.W. Hell, 4Pi-confocal images with axial superresolution, J. Microsc. 183 (1996) 189–193.
[172] S.W. Hell, M. Schrader, H.T.M. van der Voort, Far-field fluorescence microscopy with three-dimensional resolution in the 100 nm range, J. Microsc. 185 (1997) 1–5.
[173] M.G.L. Gustafsson, D.A. Agard, J.W. Sedat, I5M: 3D widefield light microscopy with better than 100 nm axial resolution, J. Microsc. 195 (1999) 10–16.
[174] H. Gugel, J. Bewersdorf, S. Jakobs, J. Engelhardt, R. Storz, S.W. Hell, Cooperative 4Pi excitation and detection yields sevenfold sharper optical sections in live-cell microscopy, Biophys. J. 87 (2004) 4146–4152.
[175] A. Egner, S. Verrier, A. Goroshkov, H.D. Soling, S.W. Hell, 4Pi-microscopy of the Golgi apparatus in live mammalian cells, J. Struct. Biol. 147 (2004) 70–76.
[176] A. Egner, S.W. Hell, Fluorescence microscopy with super-resolved optical sections, Trends Cell Biol. 15 (2005) 207–215.
[177] K. Bahlmann, S. Jakobs, S.W. Hell, 4Pi-confocal microscopy of live cells, Ultramicroscopy 87 (2001) 155–164.
[178] H. Kano, S. Jakobs, M. Nagorni, S.W. Hell, Dual-color 4Pi-confocal microscopy with 3D-resolution in the 100 nm range, Ultramicroscopy 90 (2002) 207–213.
[179] S.W. Hell, J. Wichmann, Breaking the diffraction resolution limit by stimulated emission: stimulated emission depletion microscopy, Opt. Lett. 19 (1994) 780–782.
[180] S.W. Hell, M. Kroug, Ground-state depletion fluorescence microscopy, a concept for breaking the diffraction resolution limit, Appl. Phys., B 60 (1995) 495–497.
[181] S.W. Hell, Increasing the resolution of far-field fluorescence light microscopy by point-spread-function engineering, in: J.R. Lakowicz (Ed.), Topics in Fluorescence Spectroscopy, Plenum Press, New York, 1997, pp. 361–422.
[182] S.W. Hell, S. Jakobs, L. Kastrup, Imaging and writing at the nanoscale with focused visible light through saturable optical transitions, Appl. Phys., A 77 (2003) 859–860.
[183] T.A. Klar, S. Jakobs, M. Dyba, A. Egner, S.W. Hell, Fluorescence microscopy with diffraction resolution barrier broken by stimulated emission, Proc. Natl. Acad. Sci. U. S. A. 97 (2000) 8206–8210.
[184] M. Dyba, S. Jakobs, S.W. Hell, Immunofluorescence stimulated emission depletion microscopy, Nat. Biotechnol. 21 (2003) 1303–1304.
[185] K.I. Willig, S.O. Rizzoli, V. Westphal, R. Jahn, S.W. Hell, STED-microscopy reveals that synaptotagmin remains clustered after synaptic vesicle exocytosis, Nature 440 (2006) 935–939.
[186] R. Heintzmann, T.M. Jovin, C. Cremer, Saturated patterned excitation microscopy—A concept for optical resolution improvement, J. Opt. Soc. Am. A 19 (2002) 1599–1609.
[187] M.G. Gustafsson, Nonlinear structured-illumination microscopy: wide-field fluorescence imaging with theoretically unlimited resolution, Proc. Natl. Acad. Sci. U. S. A. 102 (2005) 13081–13086.
[188] M. Hofmann, C. Eggeling, S. Jakobs, S.W. Hell, Breaking the diffraction barrier in fluorescence microscopy at low light intensities by using reversibly photoswitchable proteins, Proc. Natl. Acad. Sci. U. S. A. 102 (2005) 17565–17569.
[189] K.A. Lukyanov, A.F. Fradkov, N.G. Gurskaya, M.V. Matz, Y.A. Labas, A.P. Savitsky, M.L. Markelov, A.G. Zaraisky, X.N. Zhao, Y. Fang, W.Y. Tan, S.A. Lukyanov, Natural animal coloration can be determined by a nonfluorescent green fluorescent protein homolog, J. Biol. Chem. 275 (2000) 25879–25882.
[190] R. Ando, H. Mizuno, A. Miyawaki, Regulated fast nucleocytoplasmic shuttling observed by reversible protein highlighting, Science 306 (2004) 1370–1373.
[191] M. Andresen, M.C. Wahl, A.C. Stiel, F. Gräter, L.V. Schäfer, S. Trowitzsch, G. Weber, C. Eggeling, H. Grubmüller, S.W. Hell, S. Jakobs, Structure and mechanism of the reversible photoswitch of a fluorescent protein, Proc. Natl. Acad. Sci. U. S. A. 102 (2005) 13070–13074.
[192] M. Dyba, S.W. Hell, Focal spots of size λ/23 open up far-field florescence microscopy at 33 nm axial resolution, Phys. Rev. Lett. 88 (2002) 163901.
[193] V. Westphal, L. Kastrup, S.W. Hell, Lateral resolution of 28 nm (λ/25) in far-field fluorescence microscopy, Appl. Phys., B 77 (2003) 377–380.